Cell Metabolism
Article

TAp63 Is a Master Transcriptional Regulator of Lipid and Glucose Metabolism

Xiaohua Su,[1] Young Jin Gi,[1] Deepavali Chakravarti,[1,2] Io Long Chan,[1] Aijun Zhang,[5] Xuefeng Xia,[5] Kenneth Y. Tsai,[2,3,4] and Elsa R. Flores[1,2,*]
[1]Department of Biochemistry and Molecular Biology
[2]Graduate School of Biomedical Sciences
[3]Department of Immunology
[4]Department of Dermatology
The University of Texas M.D. Anderson Cancer Center, 1515 Holcombe Boulevard, Houston, TX 77030, USA
[5]Diabetes Research Center, Methodist Hospital Research Institute, 6565 Fannin Street, Houston, TX 77030 USA
*Correspondence: elsaflores@mdanderson.org
http://dx.doi.org/10.1016/j.cmet.2012.09.006

SUMMARY

TAp63 prevents premature aging, suggesting a link to genes that regulate longevity. Further characterization of *TAp63−/−* mice revealed that these mice develop obesity, insulin resistance, and glucose intolerance similar to those seen in mice lacking two key metabolic regulators, *Silent information regulator T1* (*Sirt1*) and *AMPK*. While the roles of Sirt1 and AMPK in metabolism have been well studied, their upstream regulators are not well understood. We found that TAp63 is important in regulating energy metabolism by accumulating in response to metabolic stress and transcriptionally activating *Sirt1*, *AMPKα2*, and *LKB1*, resulting in increased fatty acid synthesis and decreased fatty acid oxidation. Moreover, we found that TAp63 lowers blood glucose levels in response to metformin. Restoration of Sirt1, AMPKα2, and LKB1 in *TAp63−/−* mice rescued some of the metabolic defects of the *TAp63−/−* mice. Our study defines a role for TAp63 in metabolism and weight control.

INTRODUCTION

Obesity is a global health problem, and obesity-related diseases such as diabetes and heart disease are a critical threat to human longevity (Banks et al., 2008; Flegal et al., 2005). The sirtuin family of genes is an important regulator of longevity in multiple organisms from yeast to mice (Haigis and Guarente, 2006; Kume et al., 2010; Lin et al., 2000; Rogina and Helfand, 2004). Sirt1 is one of seven sirtuin members in mammals and has received a flurry of attention based on its ability to regulate synthesis, storage, and utilization of lipids (Rodgers and Puigserver, 2007; Takemori et al., 2011). Transgenic and knockout mice of *Sirt1* have phenotypes that have revealed critical clues about its function in aging, metabolism, and cancer. For example, *Sirt1* transgenic mice are protected from glucose intolerance and have a more active metabolism and leaner bodies (Banks et al., 2008). Tissue-specific deletion in liver and brain of *Sirt1* in mice resulted in increased body weight, fatty liver, and glucose intolerance associated with aging (Cohen et al., 2009; Purushotham et al., 2009). *Sirt1* also plays an important role in cancer and has been shown to regulate genes involved in senescence, DNA repair, and tumor suppression (Wang et al., 2008).

Recent reports have indicated an interdependence of AMP-activated protein kinase (AMPK) and Sirt1 (Cantó et al., 2010) in response to fasting and exercise. AMPK regulates energy homeostasis through its ability to balance catabolic and anabolic activity to regulate lipid and glucose metabolism (Hardie and Frenguelli, 2007; Towler and Hardie, 2007). This function of AMPK is critical for its response to metabolic stress. Importantly, AMPK activation is required for the therapeutic benefits of the drug metformin in the management of type 2 diabetes (Shaw et al., 2004, 2005). The activation of AMPK occurs through phosphorylation by the tumor suppressor and upstream kinase, LKB1 (Woods et al., 2003).

Sirt1, AMPK, and LKB1 are key metabolic regulators. Sirt1 mediates metabolic and the physical beneficial effects of caloric restriction (CR), such as the extension of life span, while AMPK stimulates fatty acid oxidation (Boily et al., 2008; Cantó et al., 2010), and LKB1 is a regulator of AMPK. The mechanistic regulation of these functions of Sirt1 and AMPK is primarily through their ability to posttranslationally modify transcription factors, such as FOXO1, p53, and acetyl-CoA carboxylase (ACC1), thereby affecting their downstream functions (Banks et al., 2008; Cantó et al., 2009; Rodgers et al., 2005; Vaziri et al., 2001). Sirt1 directly deacetylates p53 and AMPK phosphorylates ACC1. The phosphorylation of ACC1 is critical for the production of malonyl-CoA as a substrate for fatty acid biosynthesis. While it is clear that Sirt1, AMPK, and LKB1 play crucial roles in energy metabolism in response to different energy stresses, how they are regulated in response to metabolic stress remains unclear.

Recently, we demonstrated that the *p53* family member and *p63* isoform, *TAp63*, plays critical roles in aging and in the suppression of tumorigenesis and metastasis (Flores et al., 2005; Su et al., 2009, 2010). The vast majority of research on p63 has been performed using mouse models deficient for all isoforms of *p63* (Mills et al., 1999; Yang et al., 1999). Using these mouse models, p63 has been found to be critical for epidermal

morphogenesis (Mills et al., 1999; Yang et al., 1999). The generation of isoform-specific knockout mice for p53 family members has unveiled unique functions for these genes (Guo et al., 2009; Su et al., 2009, 2010; Suh et al., 2006). We have generated *TAp63*−/− mice and have found that *TAp63*−/− mice age prematurely, and TAp63 is critical for the maintenance of adult stem cells in quiescence (Su et al., 2009). Loss of *TAp63* triggers a senescence program in *TAp63*-deficient tissues, resulting in premature aging and reduced life span in mice (Guo et al., 2009; Su et al., 2009). We also found that *TAp63*+/− and *TAp63*−/− are highly tumor prone and develop metastatic disease (Su et al., 2010). Here, we show that in addition to these phenotypes, aging *TAp63*−/− mice develop multiple phenotypes consistent with type 2 diabetes, including glucose intolerance, insulin resistance, and liver steatosis (fatty liver). These mice phenocopy those with tissue-specific deletions of *Sirt1* as well as those deficient for *AMPKα* (Cohen et al., 2009; Purushotham et al., 2009; Viollet et al., 2003). Moreover, we found that TAp63 upregulates Sirt1 after calorie restriction. We found that the mechanism for these phenotypes is the requirement for TAp63-mediated transcriptional activation of *Sirt1*, *AMPKα2*, and *LKB1*. Consistent with regulation of *AMPKα2* and *LKB1* by TAp63, we found that TAp63 is critical for lowering blood glucose levels in response to metformin, a drug used to treat type 2 diabetes. These findings reveal roles for TAp63 in metabolism and indicate that TAp63 is a potential therapeutic target for metabolic disorders.

RESULTS

TAp63–/– Mice Develop Obesity

We observed that as *TAp63*−/− mice age they become obese by 8 months of age (Figure 1A). By 12 months of age, we observed that some mice weighed as much as 91 g and were immobile and unable to access food and water (Figure 1B). We found that *TAp63*−/− mice had increased body fat that was present underneath the skin and intercalated into multiple organs (Figure 1C). To understand the role of *TAp63* in obesity, we aged a cohort of 15 mice for 18 months and found that by 8 months of age, the *TAp63*−/− mice weighed 30% more than their wild-type (WT) littermates (Figure 1D). This difference increased to 40% by 12 months of age (Figure 1D).

To systematically assess weight gain in the *TAp63*−/− mice, we maintained 15 *TAp63*−/− and 15 WT mice on a high-fat (HF) diet for 16 weeks beginning at 4 weeks of age. A similar number of WT and *TAp63*−/− mice were fed a control (con) or CR diet. We found that as early as 2 weeks after being shifted to a HF diet, the *TAp63*−/− mice exhibited significant weight gain as compared to WT mice (Figure 1E). *TAp63*−/− mice fed control or CR diets had body weights that were comparable to their WT counterparts throughout the experiment (Figure 1E), indicating that *TAp63* is critical for regulating weight when mice are challenged with HF diets. This was not due to increased food intake, since we found no significant difference in the amount of food consumed by *TAp63*−/− mice compared to WT mice on all three diets (Figures 1F and 1G and data not shown).

To determine whether the weight gain in the *TAp63*−/− mice could be attributed to differences in activity, we compared the horizontal activity of five WT and five *TAp63*−/− mice over a 24 hr period and found the activity of the *TAp63*−/− mice is significantly lower than their WT littermates (Figure 1H). We also measured levels of oxygen consumed and carbon dioxide produced and found that *TAp63*−/− mice consume less oxygen (Figure 1I) and produce less carbon dioxide (Figure 1J) than their WT littermates. Moreover, we found that the respiratory quotient (RQ) is higher in *TAp63*−/− mice during the light cycle relative to WT mice, indicating a relative resistance to fatty acid metabolism (Figure 1K). Lastly, we found that heat production in *TAp63*−/− mice is significantly lower than in WT mice (Figure 1L). Taken together, these data indicate that *TAp63*−/− mice have impaired energy metabolism.

TAp63 Regulates Energy Metabolism

To determine whether *TAp63*−/− mice had defects in energy metabolism, we measured glucose tolerance and serum levels of triglycerides, cholesterol, and insulin. To determine whether *TAp63*−/− mice have decreased glucose tolerance, we challenged ten *TAp63*−/− and ten WT mice at 12 months of age with 2 g of glucose per kilogram of body weight. We found that *TAp63*−/− mice had a significantly decreased glucose tolerance as compared to WT mice (Figures 2A and 2B). To determine whether this was an age-associated phenomenon, we challenged 15 *TAp63*−/− mice with a HF diet for 16 weeks beginning at 4 weeks of age and measured the glucose tolerance of these mice after 16 weeks on the HF diet (Figures 2C and 2D). We found that young *TAp63*−/− mice on a HF diet also developed glucose intolerance (Figures 2C and 2D). Diabetes and insulin resistance are associated with defects in glucose uptake. To understand whether *TAp63*-deficient mice are defective in glucose uptake, we measured the ability of *TAp63*−/− mouse embryo fibroblasts (MEFs) to uptake glucose. Indeed, *TAp63*−/− MEFs had a dramatically reduced ability to uptake glucose (Figure 2E). Glucose intolerance and defects in glucose uptake are associated with insulin resistance and type 2 diabetes. To determine whether *TAp63*−/− mice develop insulin resistance, we measured levels of glucose in WT and *TAp63*−/− mice subsequent to insulin injection (Figure 2F) and found that *TAp63*−/− mice had significantly higher levels of glucose (Figure 2G), indicating resistance to insulin. We also found that *TAp63*−/− mice fed a control or a HF diet have significantly higher serum insulin compared with their WT littermates at 5 months of age (Figure 2H). We have shown previously that *TAp63*−/− mice exhibit signs of premature aging in some tissues (Su et al., 2009, 2010). To determine whether the metabolic defects observed in the *TAp63*−/− mice are due to premature senescence, we assayed for markers of senescence in MEFs and livers of *TAp63*−/− mice. We found that *TAp63*−/− MEFs at passage 2 had increased levels of senescence associated β-galactosidase (Figure S1A). Therefore, we used passage 1 MEFs in all of our studies. Moreover, we found that livers from *TAp63*−/− mice did not show evidence of senescence and expressed WT levels of $p16^{Ink4a}$, $p19^{Arf}$, and *PML*, indicating that premature senescence was not the cause of the metabolic defects of the *TAp63*−/− mice (Figure S1B). Taken together, these data are consistent with type 2 diabetes and other mouse models with this disease (Memon et al., 1994).

Lipid accumulation and increased plasma levels of triglycerides are associated with insulin resistance and type 2 diabetes (Ginsberg et al., 2005). *TAp63*−/− mice fed a control diet are

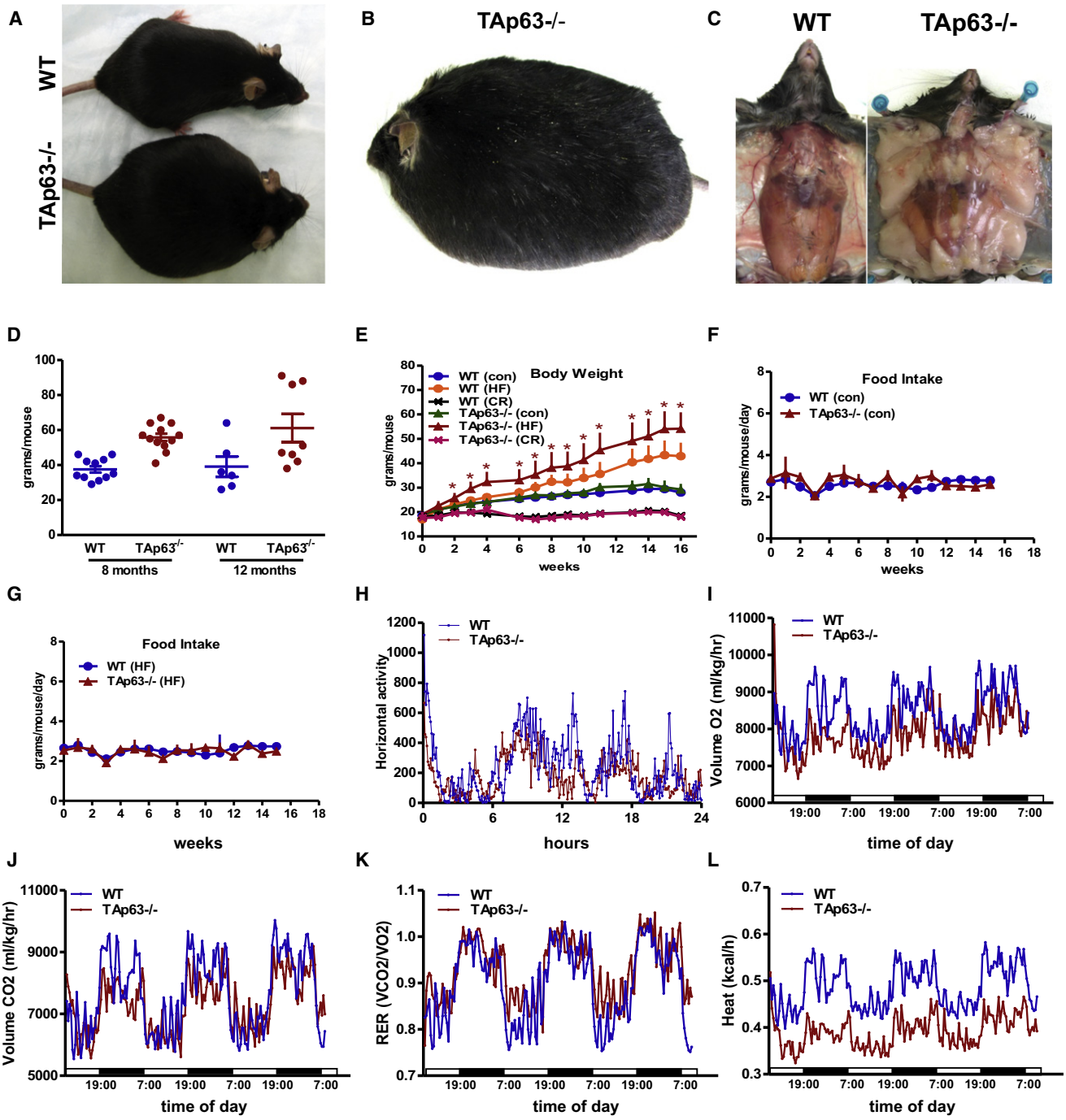

Figure 1. *TAp63–/–* Mice Develop Obesity

(A) Photograph of 8-month-old WT (WT) and *TAp63−/−* littermates.

(B) Twelve-month-old *TAp63−/−* mouse (91 g).

(C) Representative examples of fat distribution in 8-month-old WT and *TAp63−/−* mice.

(D) Body weight distribution of WT and *TAp63−/−* mice at 8 and 12 months.

(E) Weekly weight of WT and *TAp63−/−* mice fed with control or high-fat food (n = 15 per group).

(F and G) Food intake of WT and *TAp63−/−* mice fed a control diet (F) or high-fat (HF) diet (G) from 1 to 5 months of age.

(H) Horizontal activity over a 24 hr period. n = 5 for each indicated genotype.

(I–L) Indirect calorimetry of WT (blue line) and *TAp63−/−* (red line) mice: oxygen consumption (VO2) (I), carbon dioxide release (VCO2) per kg of lean body weight (J), respiratory exchange ratio (RER, VCO2/CO2) (K), or energy expenditure kcal/hour (L). n = 5 mice. Data are represented as mean ± SEM. Asterisks indicate statistical significance, $p < 0.05$.

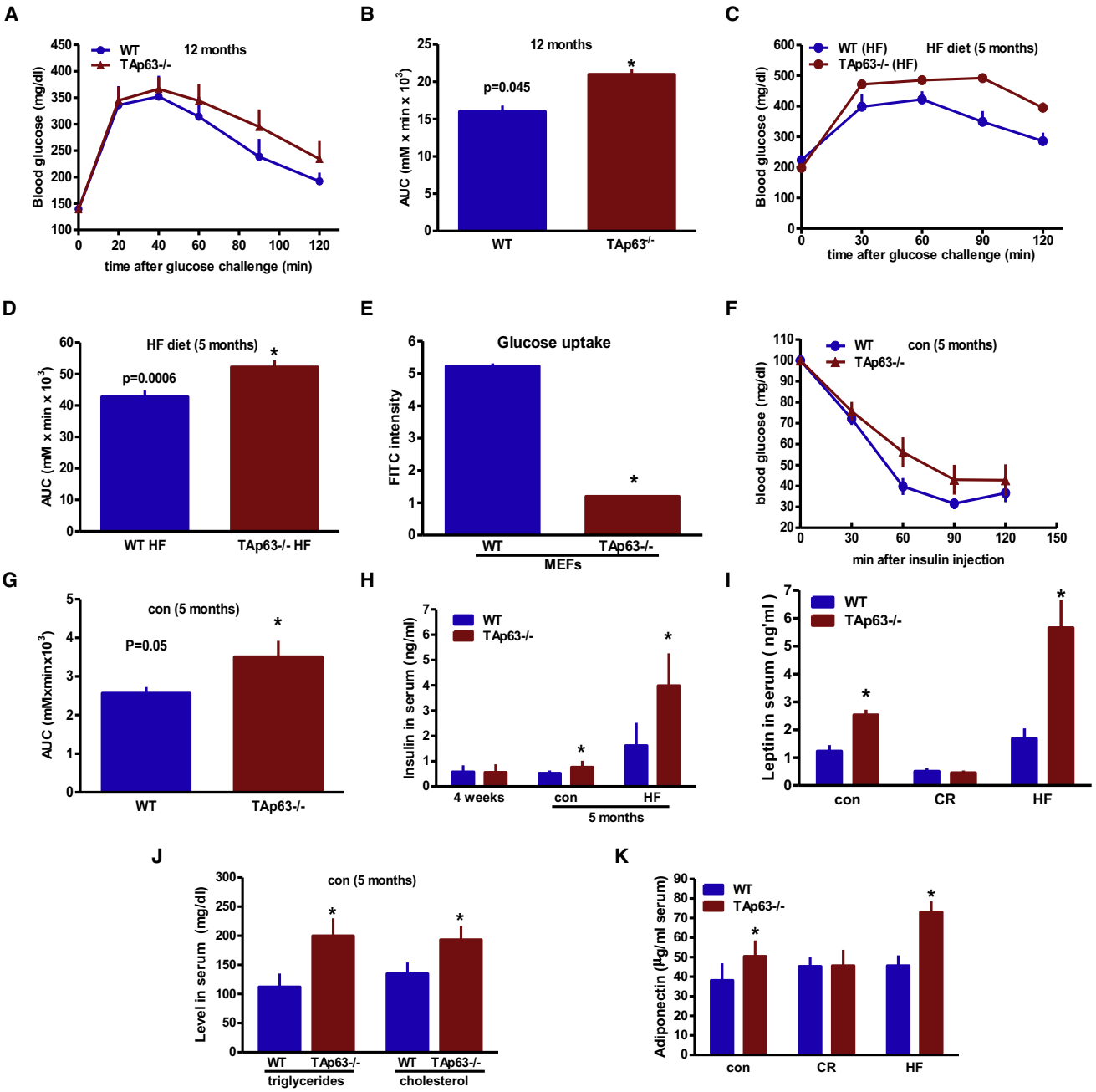

Figure 2. *TAp63–/–* Mice Are Glucose Intolerant and Insulin Resistant

(A) Glucose tolerance test performed on 12-month-old WT and *TAp63−/−* mice fasted for 18 hr (n = 10). Each point on the graph indicates the level of glucose in the blood at the indicated time point on the x axis.

(B) Areas under the curves (AUC) calculated from mice in (A). n = 10 for each genotype.

(C) Glucose tolerance test performed on 5-month-old WT and *TAp63−/−* mice fed a high-fat (HF) diet for 16 weeks (n = 15).

(D) AUC calculated from mice in (C). n = 15 for each genotype.

(E) Glucose uptake of WT and *TAp63−/−* MEFs.

(F) Insulin tolerance test performed on 5-month-old WT and *TAp63−/−* mice with control diet (n = 8).

(G) Areas under the curves (AUC) calculated from mice in (F) (n = 8).

(H) Serum insulin levels in WT and *TAp63−/−* mice at 5 months of age after being fed a HF diet for 16 weeks.

(I) Blood serum levels of leptin in WT and *TAp63−/−* mice at 5 months of age fed the indicated diet (n = 8).

(J) Serum triglyceride and cholesterol in WT and *TAp63−/−* mice at 5 months of age after being fed a control (con) diet for 16 weeks.

(K) Blood serum levels of adiponectin in WT and *TAp63−/−* mice at 5 months of age fed the indicated diet (n = 8). Data are represented as mean ± SEM. Asterisks indicate statistical significance, $p < 0.05$.

glucose intolerant and insulin resistant; therefore, we examined the levels of lipids in these mice. Blood was drawn from 15 fasting *TAp63*−/− and WT mice at 5 months of age that had been maintained on a control diet. We found that the levels of cholesterol, triglycerides, adiponectin, and leptin were significantly higher in *TAp63*−/− than in WT mice (Figures 2I–2K). These data indicate that TAp63 is important for lipid metabolism and that loss of *TAp63* leads to obesity and diabetes in mice.

TAp63−/− Mice Develop Liver Steatosis

High levels of lipids and triglycerides in the blood are associated with fat accumulation in the liver and liver steatosis (fatty liver disease). To determine whether *TAp63*−/− mice develop liver steatosis, we examined hematoxylin and eosin (H&E)-stained livers from *TAp63*−/− and WT mice (Figures 3A–3H). We found that livers from 12-month-old *TAp63*−/− mice fed control chow had many areas of fat deposition as compared to livers from WT mice of the same age (Figures 3A and 3E). Even livers from young *TAp63*−/− mice at 5 months of age that were fed control, CR, and HF diets for 16 weeks beginning at 4 weeks of age exhibited a higher accumulation of fat than their WT counterparts (compare Figures 3B and 3F, Figures 3C and 3G, and Figures 3D and 3H). This was further demonstrated by oil red O staining showing accumulation of lipids in the livers of *TAp63*−/− mice (compare Figures 3I and 3M, Figures 3J and 3N, Figures 3K and 3O, and Figures 3L and 3P). These data indicate that lipids accumulate in the tissues of *TAp63*−/− mice.

Increased lipid deposition in the blood, liver, and other tissues can be caused by increased fatty acid synthesis, decreased utilization of lipids, or both. To determine whether levels of important regulators of lipid homeostasis were affected in the absence of *TAp63*, we measured mRNA levels derived from livers of 5-month-old *TAp63*-deficient mice fed a control diet for fatty acid synthase (FAS), an enzyme that catalyzes fatty acid synthesis, leading to increased incorporation of free fatty acids into triglycerides (Figure 3Q), and carnitine palmitoyltransferase-1 (*CPT-1*) (Figure 3R), a rate-limiting enzyme for fatty acid oxidation. We found that the mRNA levels were altered in livers from *TAp63*−/− mice compared to WT mice, suggesting that the increase in the levels of lipids in *TAp63*-deficient mice is due to deregulation of these metabolic enzymes. Moreover, we examined a panel of genes involved in lipid storage and metabolism and found that expression of these mRNAs is deregulated in the absence of *TAp63* (Figure 3S).

To determine the contribution of *CPT-1* deregulation to lipid metabolism and mitochondrial dysfunction in *TAp63*-deficient mice, we measured the oxygen consumption rate in control and *TAp63*−/− MEFs under basal conditions and in response to palmitate, the substrate of CPT-1. *TAp63*−/− MEFs exhibited low basal mitochondrial oxygen consumption (Figure 3T) and an impaired ability to metabolize palmitate (Figure 3U). These data indicate that *TAp63*−/− mice have defects in both fatty acid accumulation and fatty acid oxidation. On the basis of these findings, we conclude that fatty acid synthesis is increased and fatty oxidation is decreased in *TAp63*−/− mice.

TAp63 Regulates the Sirt1/AMPK/LKB1 Pathway

The altered expression of enzymes regulated by silent information regulator T1 (Sirt1) and/or AMPKα in *TAp63*-deficient mice (Figures 3Q–3S) led us to ask whether TAp63 regulates lipid metabolism through Sirt1, AMPK, or LKB1. We measured the protein and mRNA levels of these energy sensors and metabolism regulators in tissues from *TAp63*-deficient mice at 4 weeks and 5 months of age. We found that MEFs (Figure 4A) and muscle from 4-week-old *TAp63*−/− mice have lower levels of Sirt1 than their WT counterparts, while liver fat and skin showed no significant difference (Figure 4B). Importantly, we found that levels of Sirt1 are unchanged in the skin of *TAp63*−/− mice (Figure 4B), suggesting that TAp63 regulates Sirt1 expression in metabolic tissues. In contrast, by 5 months of age, we could see that Sirt1 is lower in muscle, fat, and liver. This difference could also be seen in tissues from *TAp63*−/− mice fed a control (con) or CR diet (Figures 4C–4E). When *TAp63*−/− mice were fed a HF diet, Sirt1 levels were only found to be lower in fat (Figures 4C–4E).

Levels of Sirt1 are upregulated in response to CR through a mechanism that is not clearly understood, and levels of Sirt1 decline with age (Brooks and Gu, 2009). To determine whether TAp63 is required for Sirt1 upregulation in response to CR, we measured the levels of Sirt1 in the livers of 5-month-old WT and *TAp63*−/− mice that had been on a CR diet for 16 weeks beginning at 4 weeks of age. At this age, levels of Sirt1 were lower in muscle and fat of *TAp63*−/− mice compared to WT mice (Figures 4C–4E). These data indicate a role for *TAp63* in Sirt1 upregulation in response to CR in certain tissues, like muscle and fat. Sirt1 is known to deacetylate p53. To ask whether p53 is deacetylated by Sirt1 in the absence of *TAp63* where levels of Sirt1 are low, we performed western blot analysis for acetylated p53 in the muscle, fat, and livers of *TAp63*−/− mice fed a con, CR, or HF diet. We found that in all cases there is an increase in p53 acetylation (Figure 4C), indicating that Sirt1 in not functional in the absence of *TAp63*.

To determine if the difference occurred at the transcriptional level, we assayed the levels of *Sirt1* mRNA in WT and *TAp63*−/− MEFs starved for 6 hr. We found that while levels of *Sirt1* are upregulated in WT MEFs, the levels of *Sirt1* remain unchanged in *TAp63*−/− MEFs, suggesting that TAp63 is required for upregulation of *Sirt1* in response to glucose starvation (Figure 4F). Moreover, we found that *Sirt1* levels are upregulated in WT mice that were fasted for 18 hr, while levels of *Sirt1* do not change after this treatment in livers isolated from *TAp63*−/− mice (Figure 4G). These data indicate that TAp63 is necessary for the transcriptional upregulation of *Sirt1* in the CR response.

AMPK is another critical regulator of lipid and glucose metabolism. Activation of AMPK results in an increase in ATP production by increasing fatty acid oxidation and glucose uptake. Dysfunction of hepatic AMPK induces lipid accumulation and hyperlipidemia, which is associated with diabetes (Zang et al., 2006). Given the importance of the LKB1/AMPK in the regulation of fat oxidation and gluconeogenesis and the accumulation of lipids in the tissues from *TAp63*−/− mice, we examined the protein levels of AMPKα and LKB1 in livers from WT and *TAp63*−/− mice. We found that in 4-week-old *TAp63*−/− mice expression of AMPKα is significantly lower in muscle and fat compared to WT littermates (Figure 4H). Expression of LKB1 is lower only in the muscle of *TAp63*−/− mice at 4 weeks of age (Figure 4H). To determine whether this was an age-associated phenomenon, we assessed AMPKα and LKB1 expression in

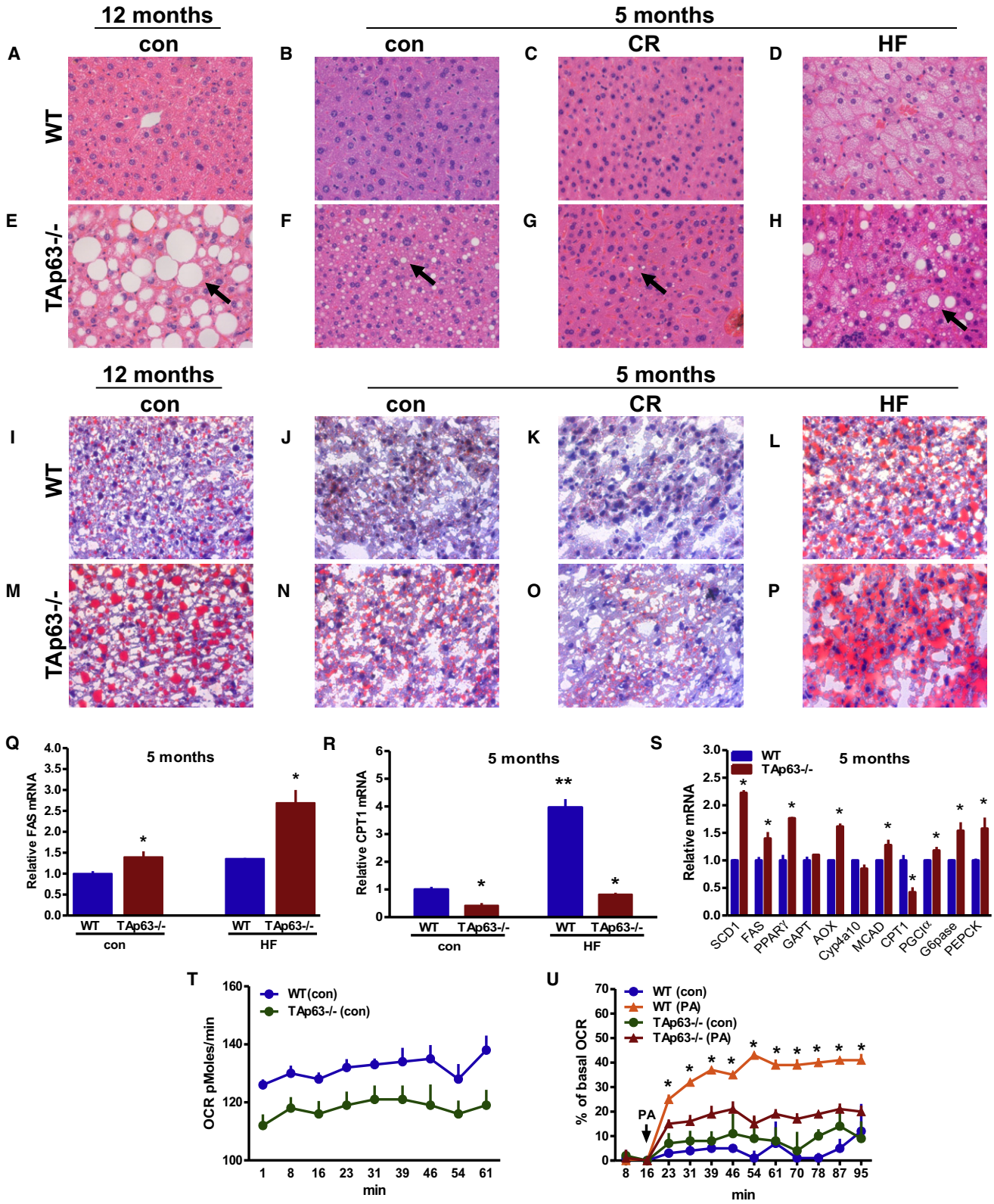

Figure 3. *TAp63–/–* Mice Display Defects in Fatty Acid Oxidation

(A–H) Hematoxylin and eosin-stained cross-sections of livers from WT (A–D) and *TAp63*−/− (E–H) mice at 12 months of age (A and E) and at 5 months of age after being fed a control (con) (B and F), calorie-restricted (CR) (C and G), or high-fat (HF) (D and H) diet for 16 weeks. Arrows indicate areas of lipid deposits. (I–P) Oil red O staining of liver from samples shown in (A–H). Red staining indicates lipid deposits.

5-month-old WT and *TAp63*−/− mice fed control, CR, or HF diets. We found that AMPKα is low in muscle, fat, and liver of *TAp63*−/− mice fed a control or CR diet (Figures 4I–4K). Five-month-old *TAp63*−/− mice fed a HF diet expressed low levels of AMPKα in fat and liver only and not in muscle (Figures 4I–4K). We found that LKB1 expression is lower in muscle, fat, and liver of 5-month-old *TAp63*−/− mice fed a control diet (Figures 4I–4K). When these mice were fed a CR or HF diet, significant differences in LKB1 expression were detected in fat and liver only and not in muscle (Figures 4I–4K). Taken together, these data indicate that TAp63 regulates expression of AMPKα and LKB1 in a tissue- and context-specific manner and seems to play a more significant role in fat and liver.

We next asked whether levels of the catalytic subunits of AMPK, *AMPKα1* and *AMPKα2*, were decreased in *TAp63*−/− mice (Figures 4L and 4M). We found that the level of *AMPKα2* was significantly lower in young *TAp63*−/− mice fed a control or HF diet (Figure 4L). These data suggest that *AMPKα2* is the subunit that is transcriptionally regulated by TAp63 in the liver.

To determine whether metabolic defects led to defects in the development of metabolic tissues in *TAp63*−/− mice, we performed histological analysis and electron microscopy of cross-sections of fat and muscle (Figure S2). We found no significant differences between these tissues in WT and *TAp63*−/− mice (Figure S2).

TAp63 Is Critical for the Response to Metformin

Previous studies have shown that AMPKα is phosphorylated and activated by the tumor suppressor and upstream kinase, LKB1, in response to metformin (Shaw et al., 2004, 2005; Woods et al., 2003). To determine whether *TAp63* is required for the response to metformin and whether AMPKα is phosphorylated in the absence of *TAp63*, we tested the activation of AMPKα and TAp63 in livers from 5-month-old WT and *TAp63*−/− mice treated with metformin. We have previously shown that TAp63γ can be activated and accumulates in response to multiple stresses, including DNA damage and wound healing (Su et al., 2009). Importantly, we found that TAp63γ accumulates in response to metformin in livers of WT mice at 5 months of age (Figure 5A). Additionally, we found that LKB1 is upregulated with a concomitant phosphorylation of AMPKα in WT livers as reported previously (Cantó et al., 2010; Shaw et al., 2004, 2005; Woods et al., 2003), while no such regulation occurred in the absence of *TAp63* (Figure 5A). We also measured phosphorylation of a downstream target of AMPK, acetyl-CoA carboxylase, ACC1, and found that levels of phosphorylated ACC1 are significantly lower in livers of *TAp63*−/− mice (Figure 5B), indicating that AMPKα is functionally inactive in the absence of *TAp63.* To further investigate the kinetics of the regulation of the LKB1-AMPK pathway by TAp63, we measured protein expression of TAp63, LKB1, and phosphorylated AMPKα in AML-12 hepatocytes after treatment with metformin for 30 min, 2 hr, 6 hr, and 24 hr. We found that TAp63γ accumulates 30 min after treatment with metformin with a concomitant phosphorylation of AMPKα (Figure 5C). Importantly, we also found that levels of TAp63γ accumulate in vivo, in mouse livers, 1 hr after metformin treatment, with peak expression at 2 hr. High expression of TAp63γ correlated with peak expression of LKB1 and phosphorylation of AMPKα in WT mice (Figure 5D). We did note that in 5-month-old *TAp63*−/− mice there was not a significant increase in LKB1 (Figure 5A), while in young 4-week-old *TAp63*−/− mice there was still an increase in LKB1 (Figure 5D), indicating an age-related factor in TAp63's ability to regulate LKB1 in response to metformin. These data indicate that TAp63 is required for LKB1 activation and downstream phosphorylation of AMPKα in response to metformin in older mice.

Because TAp63 deficiency leads to a blunted activation of the LKB1-AMPK pathway, we next asked whether metformin could lower blood glucose levels in *TAp63*−/− mice. We treated eight WT and *TAp63*−/− mice at 4 weeks of age with 250 mg/kg body weight of metformin. We found significantly higher levels of glucose in the blood of *TAp63*−/− mice compared to WT mice (Figure 5E), indicating a poor response to metformin in the absence of *TAp63*. Taken together, these data indicate that TAp63γ responds to metformin and is critical for the downstream responses that regulate glucose levels and utilization.

TAp63 Transcriptionally Activates *Sirt1*, *AMPKα2*, and *LKB1*

We observed low levels of Sirt1, AMPKα, and LKB1 in the absence of *TAp63*, suggesting that they may be transcriptionally regulated by TAp63. To determine if this is the case, we performed chromatin immunoprecipitation (ChIP) and *Luciferase* reporter gene assays. We identified a putative p63 response element within the *Sirt1* promoter located 2,016 nucleotides upstream of the start site (Table S1). Indeed, in a ChIP assay, we found that TAp63 binds to this response element, but not a nonspecific binding site located 2,000 nucleotides upstream of the p63 binding site (Figure 6A). We next performed a *Luciferase* reporter gene assay and found that the TAp63β and γ isoforms can activate the *Sirt1-luciferase* reporter gene 4–5 times over vector alone (Figures 6B and 6C). p53 and TAp63α were unable to activate this reporter gene (Figure 6C). To confirm the specificity of the identified p63 binding site on the *Sirt1* promoter, we generated a *Sirt1-luciferase* reporter gene with a mutated p63 binding site (Figure 6B). The p63 isoforms were unable to activate this reporter gene and an additional *luciferase* reporter gene with a nonspecific p63 binding site (Figures 6B and 6C). These data indicate that TAp63 binds to the *Sirt1* promoter and can transcriptionally activate it and that

(Q) Quantitative real-time PCR (qRT-PCR) analysis of *FAS* from total RNA isolated from livers of WT and *TAp63*−/− mice, n = 3.
(R) qRT-PCR analysis of *CPT-1* from mRNA isolated from livers of WT and *TAp63*−/− mice fed a con or HF diet for 16 weeks (n = 3).
(S) qRT-PCR analysis of lipid synthesis, oxidation, and gluconeogenesis pathway genes from mRNA isolated from livers of control diet WT and *TAp63*−/− mice after fasting for 18 hr (n = 3).
(T) Linear graph showing basal oxygen consumption rate (OCR) in WT and *TAp63*−/− MEFs.
(U) Oxygen consumption rate (OCR) in WT and *TAp63*−/− MEFs in response to palmitate. Arrow indicates addition of palmitate (PA). Data are represented as mean ± SEM. Asterisks indicate statistical significance, $p < 0.05$. Double asterisks indicate significant difference between WT con and WT HF groups in (R).

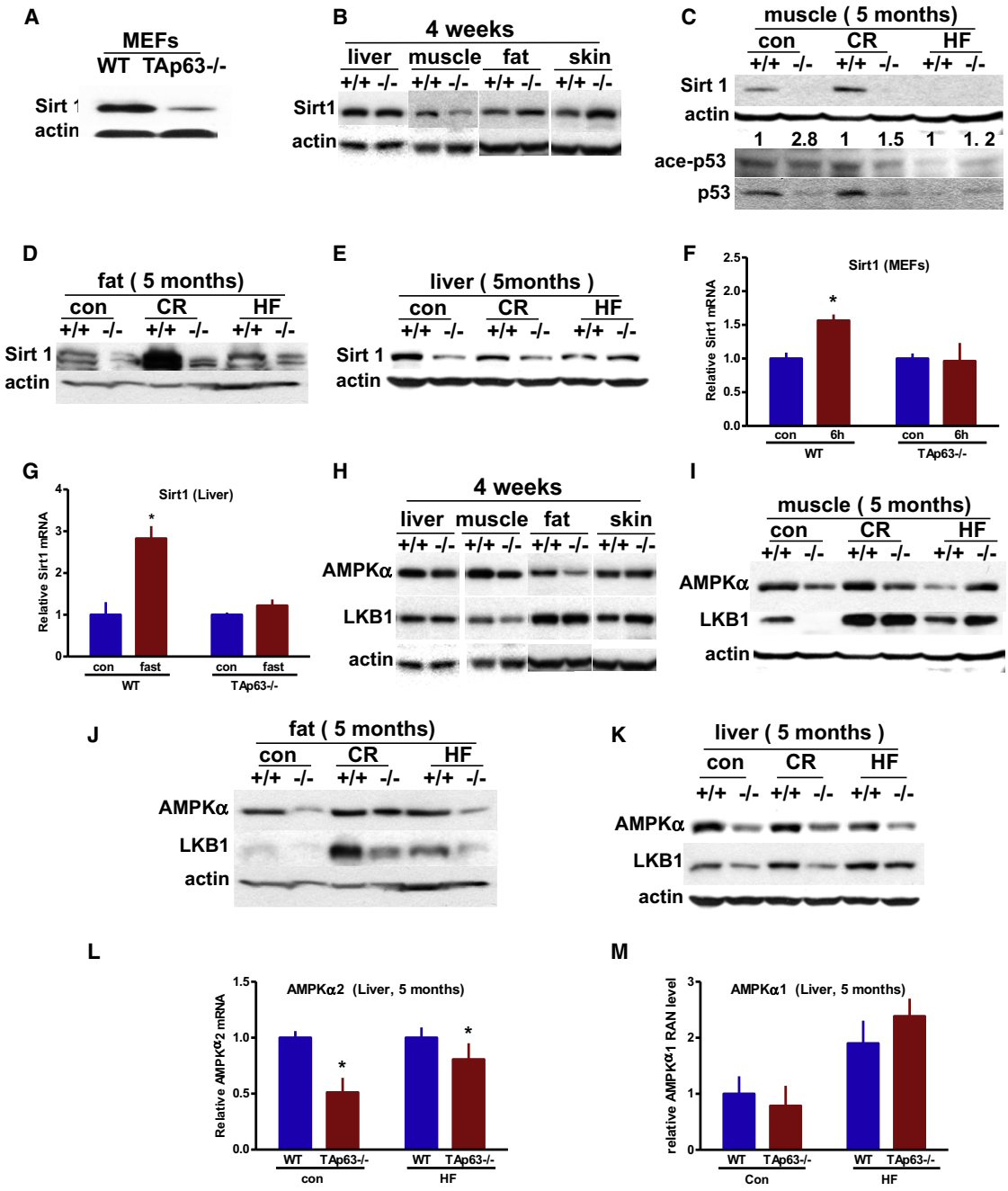

Figure 4. *Sirt1*, *AMPK*, and *LKB1* Expression in *TAp63*-Deficient Mice

(A–E) Western blot for Sirt1 using lysates extracted from: WT and *TAp63*−/− MEFs (A); liver, muscle, fat, and skin from mice at 4 weeks of age fed a control diet (B); or the indicated tissues from 5-month-old mice fed a control (con), calorie-restricted (CR), or high-fat (HF) diet for 16 weeks (C–E).

(F and G) qRT-PCR for *Sirt1* using RNA extracted from: glucose-starved MEFs (F) or livers of WT and *TAp63*−/− mice before (con) and 18 hr after fasting (fast) (G).

(H–K) Western blot for AMPKα using lysates from the indicated WT and *TAp63*−/− tissues extracted from mice at 4 weeks of age (H) or from lysates extracted from the indicated tissues of mice at 5 months of age fed a control (con), calorie-restricted (CR), or high-fat (HF) diet for 16 weeks (I–K).

(L and M) qRT-PCR for *AMPKα2* (L) and *AMPKα1* (M) in livers of WT and *TAp63*−/− mice at 5 months of age after being fed a con or HF diet for 16 weeks. Data are represented as mean ± SEM. Asterisks indicate statistical significance, $p < 0.05$.

this regulation may be critical for Sirt1 to activate the CR response.

Importantly, we also found that *AMPKα2* mRNA and protein levels are significantly lower in metabolic tissues from *TAp63*−/− mice compared to their WT counterparts (Figures 4H–4M). To determine whether TAp63 is a transcriptional regulator of *AMPKα2,* we performed ChIP and *luciferase* analyses. We identified a TAp63 binding site 1,235 nucleotides upstream

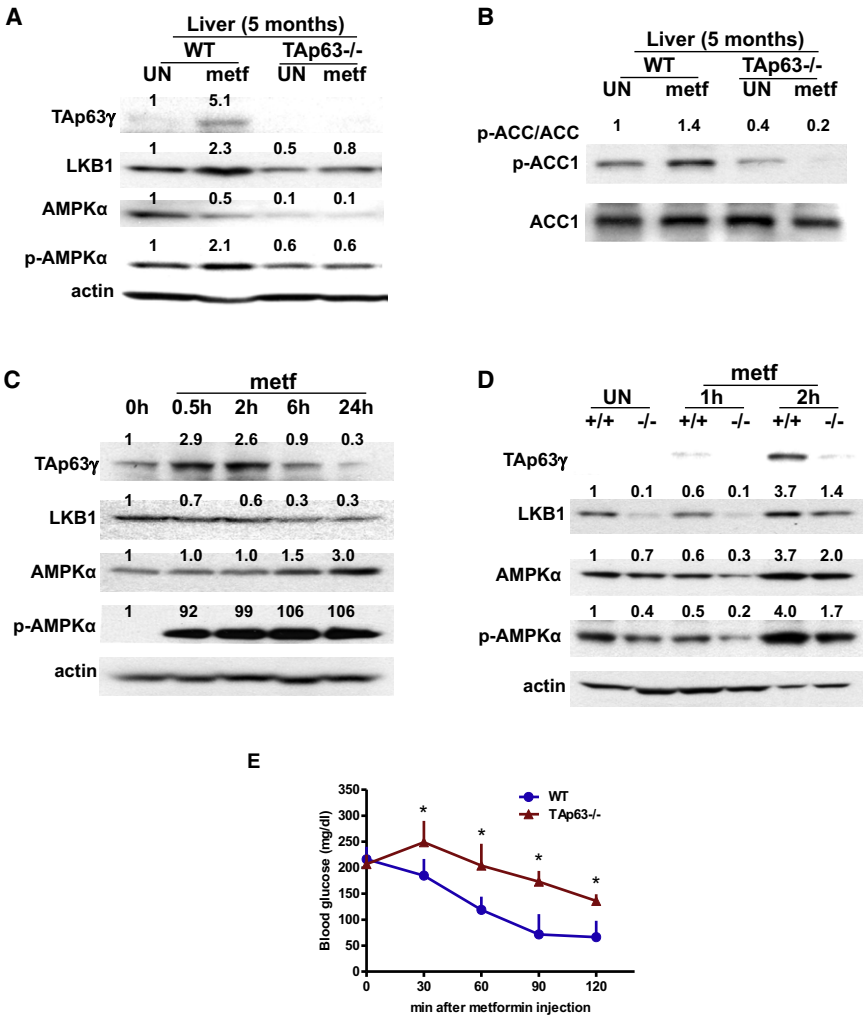

Figure 5. TAp63 Is Required for the Response to Metformin

(A and B) Western blot analysis of lysates from livers of WT and *TAp63*−/− mice at 5 months of age before (UN) and after metformin (metf) injection using the indicated antibodies.

(C and D) Western blot analysis of lysates from AML-12 cells (C) or livers from WT (+/+) and *TAp63*−/− (−/−) mice at 4 weeks of age (D) after treatment with metformin at the indicated time points using the indicated antibodies. Numbers above each western blot were measured and quantified by densitometry.

(E) Blood glucose levels in WT and *TAp63*−/− mice after metformin injection. Measurements were plotted at 30 min intervals for 2 hr, n = 8. Data are represented as mean ± SEM. Asterisks indicate statistical significance, $p < 0.05$.

of the start site (Table S1). Interestingly, we could only detect binding of TAp63 at the *AMPKα2* promoter in cells treated with 1 mM metformin, an activator of AMPK and a drug used to treat type 2 diabetes, suggesting that TAp63 may activate the AMPK pathway in response to metformin. We also found that TAp63β and γ isoforms can activate an *AMPKα2-luciferase* reporter gene containing the identified binding site (Figures 6D–6F). *AMPKα2-luciferase* reporter gene with mutations in the p63 binding site or a nonspecific binding site resulted in a complete abrogation of transactivation (Figures 6E and 6F). These data indicate that TAp63 is a transcriptional activator of *AMPKα2* and that this regulation may be critical for the regulation of energy metabolism.

LKB1 protein expression was also found to be significantly lower in *TAp63*−/− mice (Figures 4H–4K). To determine whether TAp63 is a transcriptional regulator of *LKB1*, we again performed ChIP (Figure 6G) and *luciferase* analyses (Figures 6H and 6I) and found a TAp63 binding site within intron 1 of *LKB1* (Table S1). This site was activated by TAp63α and TAp63β in *luciferase* reporter assays (Figure 6I). Taken together, these data indicate that TAp63 can bind to the *Sirt1*, *AMPKα2*, and *LKB1* promoters and can transcriptionally activate them.

We also examined the ability for TAp63 to bind to the *Sirt1*, *AMPKα2*, and *LKB1* promoters in hepatocytes (AML-12 cells) where we found that levels of TAp63 are upregulated in response to metformin (Figure 6J) or glucose starvation (Figure 6K). In AML-12 cells, we found that TAp63γ is upregulated in response to metformin (Figure 6J), resulting in binding to the *Sirt1* (Figure 6L), *AMPKα2* (Figure 6M), and *LKB1* promoters (Figure 6N). Additionally, we found that TAp63γ is upregulated in AML-12 hepatocytes in response to glucose starvation (Figure 6K), resulting in binding to the *Sirt1* (Figure 6O), *AMPKα2* (Figure 6P), and *LKB1* promoters (Figure 6Q). These data indicate that metabolic stress such as starvation or addition of metformin results in upregulation of TAp63γ and downstream transcriptional regulation of these key metabolic regulators.

TAp63 Upregulates Sirt1 in Response to Calorie Restriction

We have shown that TAp63 transcriptionally activates *Sirt1* (Figures 6A–6C, 6L, and 6O). Sirt1 is an important regulator in the response to CR by regulating the expression of *PEPCK* and *GLS2* (a gene that encodes a mitochondrial glutaminase catalyzing the hydrolysis of glutamine to glutamate), two critical enzymes for mice to adapt to CR. Given the low levels of Sirt1 in tissues from *TAp63*-deficient mice, we tested the CR response in *TAp63*−/− mice. To do this, we fed 15 *TAp63*−/− and WT mice a CR diet beginning at 4 weeks of age. After 16 weeks of being fed a CR diet, we measured fasting levels of triglycerides and glucose in blood from these mice (Figures S3A and S3B). Importantly, we found that triglycerides were elevated in *TAp63*−/− mice (Figure S3A) and that glucose levels were lower in *TAp63*−/− mice than in WT mice (Figure S3B). These data are consistent with our previous data indicating defects in fat utilization, fatty acid oxidation, and glucose utilization in the *TAp63*−/−

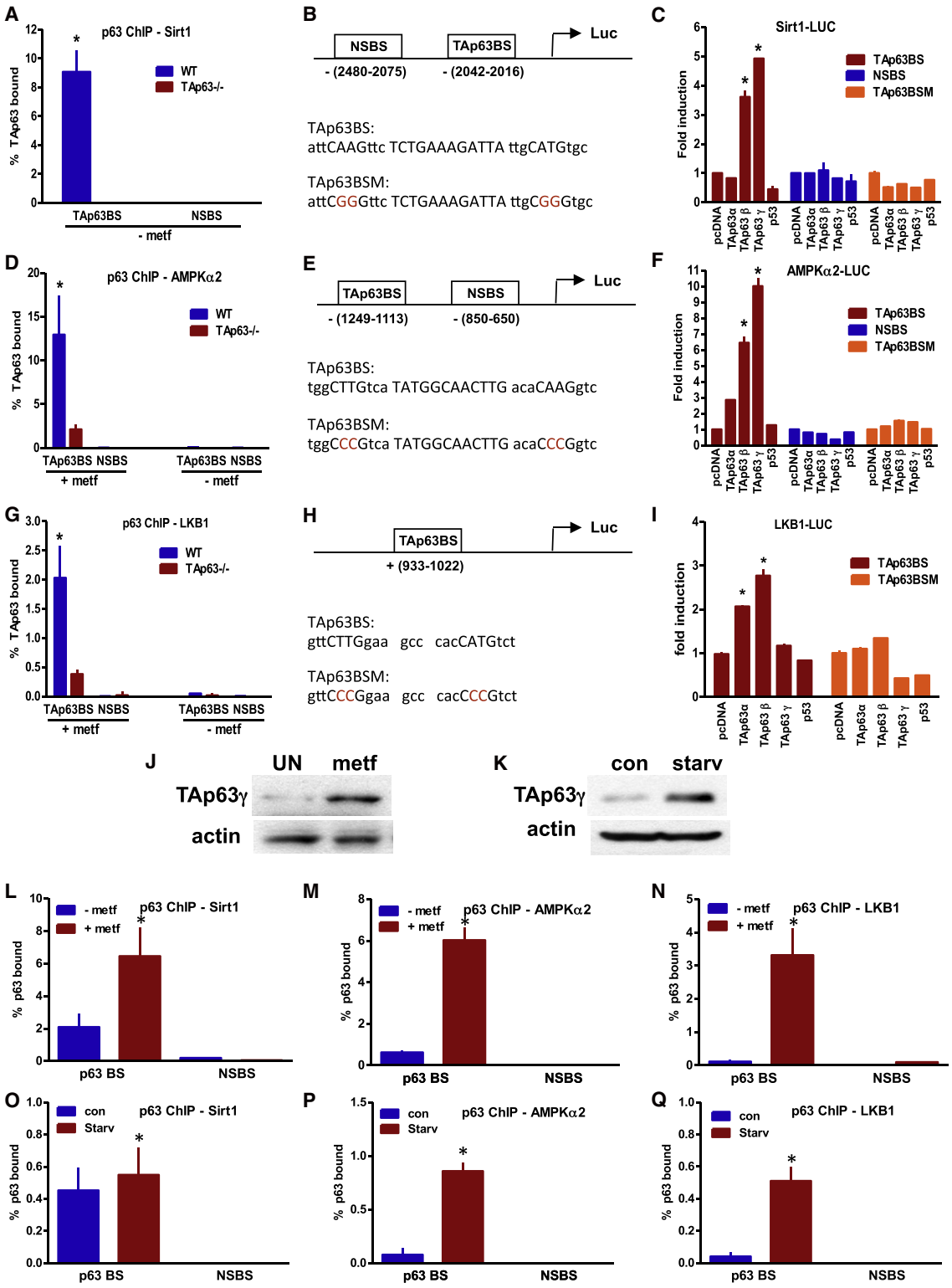

Figure 6. TAp63 Transcriptionally Activates *Sirt1*, *AMPKα2*, and *LKB1*

(A) qRT-PCR of ChIP assay using WT and *TAp63−/−* keratinocytes showing the percentage of TAp63 bound to the *Sirt1* promoter.

(B) Schematic showing TAp63 binding site (TAp63BS) on the *Sirt1* promoter and nonspecific binding site (NSBS) luciferase reporter gene. TAp63BS and a mutant of this site (TAp63BSM) are shown.

(C) Luciferase reporter gene assay for *Sirt1* in *p53−/−;p63−/−* MEFs transfected with the indicated p63 isoforms and luciferase reporter genes.

(D) qRT-PCR of ChIP assay using WT and *TAp63−/−* keratinocytes showing the percentage of TAp63 bound to the *AMPKα2* promoter.

mice (Figures 1–3). Taken together, these data demonstrate that the metabolic phenotype of the *TAp63*−/− mice is similar to that of the *Sirt1*−/− mice and that TAp63 upregulates *Sirt1* in a tissue-specific manner in response to CR.

Expression of Sirt1, AMPK, and/or LKB1 Rescues Metabolic Defects in *TAp63*−/− MEFs

To determine whether the metabolic defects observed in the *TAp63*−/− MEFs could be rescued, we transfected WT and *TAp63*−/− MEFs with vectors expressing *Sirt1*, *AMPKα2*, *LKB1*, or *Sirt1* and *LKB1* in combination (Figure S3C). To ask whether expression of these genes could rescue the defects in the mitochondria of *TAp63*−/− MEFs, we measured mitochondrial membrane potential using the JC-1 assay. We found that expression of Sirt1 or AMPKα2 partially rescues the mitochondrial defect while expression of both Sirt1 and AMPKα2 completely rescue the mitochondrial defect of the *TAp63*−/− MEFs (Figure S3D). We also asked whether the rate of basal oxygen consumption in *TAp63*−/− MEFs could be restored to WT levels by expression of Sirt1, AMPKα2, or LKB1. Indeed, we found that expression of Sirt1 in *TAp63*−/− MEFs partially rescues oxygen consumption of *TAp63*−/− MEFs while expression of AMPKα2 completely rescues the defect in the *TAp63*−/− MEFs (Figure S3E). These data indicate that re-expression of Sirt1, AMPKα2, or LKB1 can rescue the defects of the *TAp63*−/− MEFs and indicate that regulation of these genes by TAp63 leads to the metabolic defects in *TAp63*-deficient cells.

Expression of Sirt1, AMPK, and/or LKB1 Rescues Metabolic Defects in *TAp63*−/− Mice at 4 Weeks of Age

To ask whether expression of Sirt1, AMPKα2, or LKB1 could rescue the defects of the *TAp63*−/− mice in vivo, we infected *TAp63*-deficient mice at 4 weeks of age with adenoviruses expressing these genes via tail vein injection (Figure 7). Expression of AMPKα2 in the livers of *TAp63*−/− mice (Figure 7A) resulted in a rescue of expression of *CPT-1*, a key regulator of fatty acid metabolism (Figures 7B and 7C). We did not see significant rescue in respiration, glucose tolerance, or fatty liver disease in the mice (Figure S4). This may be due to the age of the mice or that the method of delivery of virus to the liver is insufficient to rescue all of the phenotypes, i.e., expression of AMPKα2 needs to be expressed in muscle and fat or other tissues in the *TAp63*−/− mice to fully rescue the metabolic defects. Expression of LKB1 rescued the expression of AMPKα and phosphorylation of AMPKα in the livers of *TAp63*−/− mice (Figure 7D). We also found that STRAD is expressed at low levels in *TAp63*−/− mice, one of the other components of the LKB1-MO25-STRAD complex (Figure 7D), while no change was seen in MO25. Importantly, *TAp63*−/− mice expressing LKB1 responded to metformin, similar to their WT counterparts (Figure 7E). These data indicate that TAp63 regulates LKB1 and is critical for the response to metformin. Lastly, we found that expression of Sirt1 in *TAp63*−/− mice resulted in WT expression of PEPCK and GLS2 in the liver (Figure 7C). Also, the levels of triglycerides in the blood are restored to WT levels in *TAp63*−/− mice expressing Sirt1 (Figure 7G). Taken together, these data indicate that re-expression of Sirt1, AMPKα2, or LKB1 can rescue some of the metabolic defects of the *TAp63*−/− mice at 4 weeks of age and indicate that regulation of these genes by TAp63 is critical for lipid and glucose metabolism.

DISCUSSION

The roles of tumor suppressor genes in metabolism are an area of intense interest and research (Bensaad et al., 2006; Jones and Thompson, 2009; Matoba et al., 2006). The altered mechanisms used by cancer cells to circumvent limiting nutrients are key to the survival and growth of a tumor. Here, we show that the tumor suppressor gene and *p53* family member, *TAp63*, plays critical roles in regulating energy metabolism. We found that *TAp63*−/− mice develop obesity, glucose intolerance, and insulin resistance. The *TAp63*−/− mice have defects in fatty acid oxidation and display mitochondrial dysfunction. These phenotypes of the *TAp63*−/− mice are reminiscent of tissue-specific deletion of *Sirt1* and *AMPKα2*−/− mouse models (Cohen et al., 2009; Purushotham et al., 2009; Viollet et al., 2003). We found that TAp63 transcriptionally activates *Sirt1*, *AMPKα2*, and *LKB1*. Loss of expression of these factors leads to defects in lipid utilization, fatty acid synthesis, fatty acid oxidation, and insulin resistance. Consequently, the *TAp63*−/− mice exhibit symptoms of premature aging (Su et al., 2009), obesity, and type 2 diabetes. Importantly, we were able to rescue some of the metabolic defects of the *TAp63*−/− mice by expressing Sirt1, AMPKα, or LKB1 in the liver of *TAp63*−/− mice at 4 weeks of age. These data reveal a role for TAp63 in regulating energy metabolism and identify TAp63 as master upstream regulator of lipid and glucose metabolism. Given the extensive interaction between the p53 family members, these data have important implications for understanding how the family of *p53* tumor suppressor genes regulates metabolism in cancer cells.

(E) Schematic showing TAp63 binding site (TAp63BS) on the *AMPKα2* promoter and nonspecific binding site (NSBS) luciferase reporter gene. TAp63BS and a mutant of this site (TAp63BSM) are shown.
(F) Luciferase reporter gene assay for *AMPKα2* in *p53*−/−;*p63*−/− MEFs transfected with the indicated p63 isoforms and luciferase reporter genes.
(G) qRT-PCR of ChIP assay using WT and *TAp63*−/− keratinocytes showing the percentage of TAp63 bound to the *LKB1* promoter.
(H) Schematic showing TAp63 binding site (TAp63BS) on the *LKB1* promoter and nonspecific binding site (NSBS) luciferase reporter gene. TAp63BS and a mutant of this site (TAp63BSM) are shown.
(I) Luciferase reporter gene assay for *LKB1* in *p53*−/−;*p63*−/− MEFs transfected with the indicated p63 isoforms and luciferase reporter genes.
(J and K) Western blot analysis of lysates from AML-12 cells after treatment with metformin (J) or starvation (K).
(L–N) qRT-PCR of ChIP assay using AML-12 cells treated with metformin showing the percentage of TAp63 bound to the *Sirt1* promoter (L), *AMPKα2* promoter (M), and *LKB1* promoter (N).
(O–Q) qRT-PCR of ChIP assay using AML-12 cells before and after starvation showing the percentage of TAp63 bound to the *Sirt1* promoter (O), *AMPKα2* promoter (P), and *LKB1* promoter (Q). Data are represented as mean ± SEM. Asterisks indicate statistical significance, $p < 0.05$. Red text in panels (B, E, and H) indicates mutated sites within the binding site.

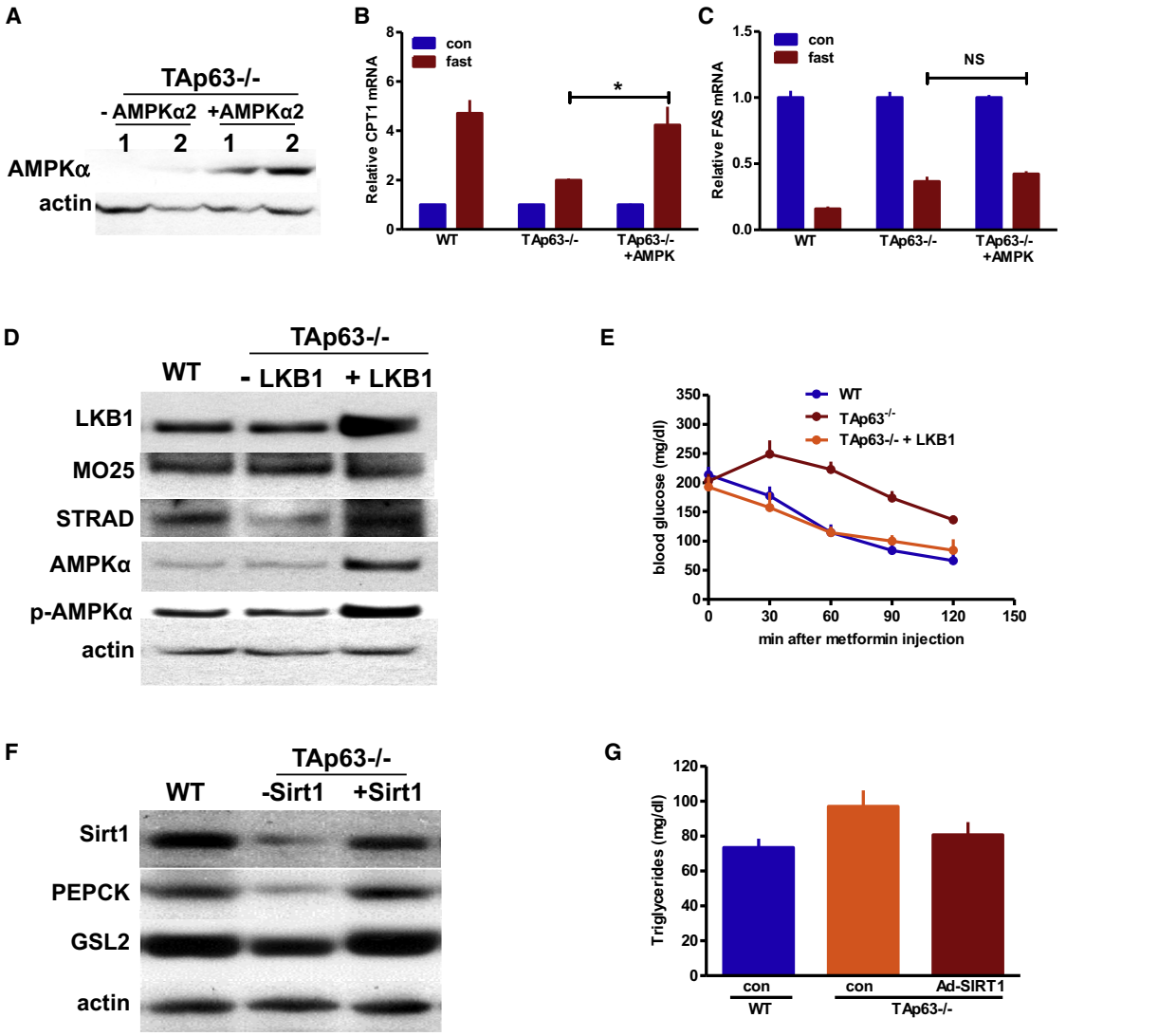

Figure 7. Expression of AMPKα2, LKB1, and Sirt1 in MEFs and Liver Rescues the Metabolic Defects of *TAp63–/–* Mice

(A) Western blot analysis of liver lysates from *TAp63*−/− mice with or without adenovirus-AMPKα2 (ad-AMPKα2) infection and using the indicated antibodies.

(B and C) Bar graph indicating qRT-PCR analysis of *CPT-1* (B), *FAS* (C) from total RNA isolated from livers of WT and *TAp63*−/− mice, and *TAp63*−/− mice expressing AMPKα2.

(D) Western blot analysis of liver lysates from WT, *TAp63*−/−, and *TAp63*−/− mice expressing LKB1 and treated with metformin using the indicated antibodies.

(E) Blood glucose levels after metformin injection of WT, *TAp63*−/−, and *TAp63*−/− mice expressing LKB1. Measurements were plotted at 30 min intervals for 2 hr.

(F) Western blot analysis of liver lysates from WT, *TAp63*−/−, and *TAp63*−/− mice expressing Sirt1 using the indicated antibodies.

(G) Serum triglyceride levels in WT, *TAp63*−/−, and *TAp63*−/− mice expressing Sirt1. Actin was used as a loading control in western blot analyses. Data are represented as mean ± SEM.

The roles of p63 have been extensively studied in epidermal morphogenesis (Mills et al., 1999; Yang et al., 1999), epidermal homeostasis (Su et al., 2009), and tumor suppression (Flores et al., 2005; Guo et al., 2009; Su et al., 2010). While the vast majority of p63 studies have been performed using mice that are deficient for all isoforms of *p63* (Mills et al., 1999; Yang et al., 1999), our *TAp63* isoform-specific knockout mice have unveiled functions for this isoform that have not been previously appreciated in studies using the *p63*−/− mice. Here we show that TAp63 is a critical transcriptional regulator of genes involved in lipid and glucose metabolism. Given the extensive interaction of the p53 family members (Flores et al., 2002, 2005; Lang et al., 2004; Olive et al., 2004), our findings have important implications for the p53 family in regulating metabolism in cancer. Previous studies have shown that *p53* plays critical roles in regulating metabolism. The primary mechanism of action of p53 in this regard is through transcriptional activation of downstream target genes. These include *TIGAR* (TP53-induced glycolysis regulator), *SCO2* (synthesis of cytochrome c oxidase) (Bensaad et al., 2006; Matoba et al., 2006), sestrin 1 and 2 (Budanov and

Karin, 2008), and AMPKβ (Feng et al., 2007). Cells within a tumor are nutrient deprived and use aerobic glycolysis as their major source of energy, the so-called Warburg effect. The switch to this mode of metabolism is critical for the survival of cells proliferating in a tumor with limited blood and oxygen. Here, we found that TAp63 transcriptionally regulates *Sirt1*, *AMPKα2*, and *LKB1* to regulate the utilization of fat and glucose. This has important implications for tumor cells with mutant p53. Mutant p53 has been shown to bind to TAp63 and inhibit its transcriptional activity (Gaiddon et al., 2001; Lang et al., 2004; Olive et al., 2004). Mice lacking *TAp63* are highly prone to metastatic tumors (Su et al., 2010) and to metabolic disorders, as we have shown here. The ability of mutant p53 to inactivate TAp63 suggests there may be interplay between p53 family members in regulating cellular metabolism in cancer. Therefore, our work has opened venues of investigation for the p53/p63/p73 field.

Consistent with a role for TAp63 in metabolic stress, we found that TAp63 responds to a drug used to treat type 2 diabetes, metformin. The levels of TAp63γ are elevated in response to metformin (Figures 5A, 5C, and 5D). In turn, levels of LKB1 increase, which not only regulates energy metabolism through its ability to phosphorylate AMPKα but is also a potent tumor suppressor gene (Shaw et al., 2004, 2005; Woods et al., 2003). Therefore, we found two modes by which TAp63 regulates AMPKα. One is through regulating the mRNA levels of *AMPKα2* itself and the other is by regulating its upstream kinase, *LKB1*. The reasons for this multilevel regulation are intriguing and areas for future research. Possible reasons for this complex regulation could be due to different cellular and metabolic stress contexts.

We have shown here that TAp63 is a critical regulator of lipid and glucose metabolism, loss of which leads to obesity and diabetes. Not only is *TAp63* a potent suppressor of tumorigenesis and metastasis (Su et al., 2010), it is also a central regulator and integrator of the metabolic response to CR and starvation. These findings provide exciting avenues of research for the p53 family and cancer fields.

EXPERIMENTAL PROCEDURES

Mice and Diet Regimen

Forty-five *TAp63*−/− and WT (WT) male mice on an enriched C57BL/6 background at 4 weeks of age were randomly assigned to three groups of 15 mice each. Each group was fed a control diet (con) (D12329, Research Diets, New Brunswick, NJ; 11% kcal from fat), HF diet (HF) (D12492, Research Diets; 60% kcal from fat), or calorie restricted diet (CR) (60% of the average daily food intake of the control group) for 16 weeks. Each mouse was housed individually. All procedures were approved by the IACUC at the University of Texas M.D. Anderson Cancer Center.

Intraperitoneal Glucose and Insulin Tolerance Test

Intraperitoneal glucose tolerance test (IPGTT) was performed by injecting D-glucose (2 g/kg body weight) intraperitoneally into mice that were fasted for 18 hr. Insulin tolerance test (ITT) was performed by injecting mice intraperitoneally with insulin (0.75 U/kg, Humulin-N from Eli Lilly) in ~0.1 ml 0.9% NaCl. Blood was collected from tail bleeds every 20–30 min over a 2 hr period, and whole-blood glucose was measured using a Precision Xtra advanced diabetes management system (MediSense). Areas under the curves for the IPGTT and ITT were calculated using PRISM5 software (GraphPad).

Metabolite Measurements

Horizontal activity, oxygen consumption rate (VO2), carbon dioxide release (VCO2), respiratory exchange ratio (RER), and heat production were measured under a consistent environmental temperature and light cycle using an indirect calorimetry system (TSE Systems). After 3 days of acclimation to the metabolic chamber, VO_2 was measured in individual mice at 5 min intervals for 72 hr. Data are normalized with respect to lean body weight. RER is the ratio of VCO_2 to VO_2. Horizontal activity was measured on x, y, and z axes by using infrared beams to count the beam breaks during a specified measurement period. Fat and lean tissue mass was determined in living, nonanesthetized mice by using a magnetic resonance imaging (MRI) at the Baylor College of Medicine Metabolism Core.

Blood Serum Measurements

Mice were fasted for 18 hr prior to collecting blood. Serum was analyzed using a Insulin Mouse Ultrasensitive ELISA kit (cat# 80-INSMSU-E01, ALPCO), Mouse Adiponectin ELISA kit (cat# CYT286, Chemicon), Mouse Leptin ELISA Kit (Millipore Lactate Reagent Kit), and the COBAS INTEGRA 400 plus System (Roche) to measure serum triglycerides and total cholesterol.

Oil Red O Staining

Frozen sections of livers from WT and *TAp63*−/− mice were fixed with 10% formalin. Oil red O (Polysciences, Inc.) staining was performed using 60% isopropanol saturated with oil red O dye for 1 hr at room temperature.

Chromatin Immunoprecipitation Assay

Keratinocytes and AML-12 hepatocytes used to assess TAp63 binding at the *AMPKα2* promoter were treated with 1 mM metformin for 6 hr. In some ChIP experiments, AML-12 cells were starved of serum and glucose for 6 hr. Anti-pan-p63 antibody (4A4, Abcam for keratinocytes, 4A4, Santa Cruz for AML-12) or IgG was used for immunoprecipitation. Putative p63 binding sites were scanned within 5,000 bp upstream of the 5′ UTR and intron 1 for the consensus p53/p63 binding site (el-Deiry et al., 1992; Su et al., 2010; Yang et al., 2006). All primers used for ChIP-PCR are listed in Table S2. ABI Step One Plus real-time PCR and SYBR green PCR master mix (Applied Biosystems) were used for quantitative real-time PCR.

In Vivo Adenoviral Gene Transfer

A total of 2×10^9 plaque-forming units (pfu) active rat Ad-AMPKα2 (Eton Bioscience), 1×10^9 pfu human Ad-LKB1 (Vector BioLabs), or 2×10^9 pfu human Ad-Sirt1 (Vector BioLabs) was injected through the tail vein of *TAp63*−/− mice. Forty-eight hours after injection, livers were collect for western blot analysis and qRT-PCR. Metformin sensitivity was measured after metformin injection (250 mg/kg) using mice infected with human Ad-LKB1.

Statistics

All data are represented as mean ± SEM. Data were analyzed using one-way ANOVA test or Student's t test for comparison between two groups. A p value of 0.05 was considered significant.

SUPPLEMENTAL INFORMATION

Supplemental Information includes four figures, two tables, and Supplemental Experimental Procedures and can be found with this article online at http://dx.doi.org/10.1016/j.cmet.2012.09.006.

ACKNOWLEDGMENTS

This work was supported by grants to E.R.F. from the American Cancer Society (RSG-07-082-01-MGO), the Mel Klein Foundation, and the Hildegardo E. and Olga M. Flores Foundation. This work was supported in part by NCI-R01 (R01CA160394), NCI-R01 (R01CA134796), and CPRIT (RP120124) to E.R.F., NCI-Cancer Center Core Grant (CA-16672) (University of Texas M.D. Anderson Cancer Center), and a Career Development Award from the Genitourinary Cancer SPORE (NCI CA091846). E.R.F. is a scholar of the Leukemia and Lymphoma Society of America, the Rita Allen Foundation, and the V Foundation for Cancer Research. D.C. was funded by a CPRIT training grant (RP101502). We would like to thank L.C.B. Chan, M.D. Saha, and P. Saha for scientific discussion and technical advice and the Mouse Metabolism Core at Baylor College of Medicine (funded by NIH P30 DK079638).

Received: October 14, 2011
Revised: May 15, 2012
Accepted: September 11, 2012
Published online: October 2, 2012

REFERENCES

Banks, A.S., Kon, N., Knight, C., Matsumoto, M., Gutiérrez-Juárez, R., Rossetti, L., Gu, W., and Accili, D. (2008). SirT1 gain of function increases energy efficiency and prevents diabetes in mice. Cell Metab. *8*, 333–341.

Bensaad, K., Tsuruta, A., Selak, M.A., Vidal, M.N., Nakano, K., Bartrons, R., Gottlieb, E., and Vousden, K.H. (2006). TIGAR, a p53-inducible regulator of glycolysis and apoptosis. Cell *126*, 107–120.

Boily, G., Seifert, E.L., Bevilacqua, L., He, X.H., Sabourin, G., Estey, C., Moffat, C., Crawford, S., Saliba, S., Jardine, K., et al. (2008). SirT1 regulates energy metabolism and response to caloric restriction in mice. PLoS ONE *3*, e1759.

Brooks, C.L., and Gu, W. (2009). How does SIRT1 affect metabolism, senescence and cancer? Nat. Rev. Cancer *9*, 123–128.

Budanov, A.V., and Karin, M. (2008). p53 target genes sestrin1 and sestrin2 connect genotoxic stress and mTOR signaling. Cell *134*, 451–460.

Cantó, C., Gerhart-Hines, Z., Feige, J.N., Lagouge, M., Noriega, L., Milne, J.C., Elliott, P.J., Puigserver, P., and Auwerx, J. (2009). AMPK regulates energy expenditure by modulating NAD+ metabolism and SIRT1 activity. Nature *458*, 1056–1060.

Cantó, C., Jiang, L.Q., Deshmukh, A.S., Mataki, C., Coste, A., Lagouge, M., Zierath, J.R., and Auwerx, J. (2010). Interdependence of AMPK and SIRT1 for metabolic adaptation to fasting and exercise in skeletal muscle. Cell Metab. *11*, 213–219.

Cohen, D.E., Supinski, A.M., Bonkowski, M.S., Donmez, G., and Guarente, L.P. (2009). Neuronal SIRT1 regulates endocrine and behavioral responses to calorie restriction. Genes Dev. *23*, 2812–2817.

el-Deiry, W.S., Kern, S.E., Pietenpol, J.A., Kinzler, K.W., and Vogelstein, B. (1992). Definition of a consensus binding site for p53. Nat. Genet. *1*, 45–49.

Feng, Z., Hu, W., de Stanchina, E., Teresky, A.K., Jin, S., Lowe, S., and Levine, A.J. (2007). The regulation of AMPK beta1, TSC2, and PTEN expression by p53: stress, cell and tissue specificity, and the role of these gene products in modulating the IGF-1-AKT-mTOR pathways. Cancer Res. *67*, 3043–3053.

Flegal, K.M., Graubard, B.I., Williamson, D.F., and Gail, M.H. (2005). Excess deaths associated with underweight, overweight, and obesity. JAMA *293*, 1861–1867.

Flores, E.R., Tsai, K.Y., Crowley, D., Sengupta, S., Yang, A., McKeon, F., and Jacks, T. (2002). p63 and p73 are required for p53-dependent apoptosis in response to DNA damage. Nature *416*, 560–564.

Flores, E.R., Sengupta, S., Miller, J.B., Newman, J.J., Bronson, R., Crowley, D., Yang, A., McKeon, F., and Jacks, T. (2005). Tumor predisposition in mice mutant for p63 and p73: evidence for broader tumor suppressor functions for the p53 family. Cancer Cell *7*, 363–373.

Gaiddon, C., Lokshin, M., Ahn, J., Zhang, T., and Prives, C. (2001). A subset of tumor-derived mutant forms of p53 down-regulate p63 and p73 through a direct interaction with the p53 core domain. Mol. Cell. Biol. *21*, 1874–1887.

Ginsberg, H.N., Zhang, Y.L., and Hernandez-Ono, A. (2005). Regulation of plasma triglycerides in insulin resistance and diabetes. Arch. Med. Res. *36*, 232–240.

Guo, X., Keyes, W.M., Papazoglu, C., Zuber, J., Li, W., Lowe, S.W., Vogel, H., and Mills, A.A. (2009). TAp63 induces senescence and suppresses tumorigenesis in vivo. Nat. Cell Biol. *11*, 1451–1457.

Haigis, M.C., and Guarente, L.P. (2006). Mammalian sirtuins—emerging roles in physiology, aging, and calorie restriction. Genes Dev. *20*, 2913–2921.

Hardie, D.G., and Frenguelli, B.G. (2007). A neural protection racket: AMPK and the GABA(B) receptor. Neuron *53*, 159–162.

Jones, R.G., and Thompson, C.B. (2009). Tumor suppressors and cell metabolism: a recipe for cancer growth. Genes Dev. *23*, 537–548.

Kume, S., Uzu, T., Horiike, K., Chin-Kanasaki, M., Isshiki, K., Araki, S., Sugimoto, T., Haneda, M., Kashiwagi, A., and Koya, D. (2010). Calorie restriction enhances cell adaptation to hypoxia through Sirt1-dependent mitochondrial autophagy in mouse aged kidney. J. Clin. Invest. *120*, 1043–1055.

Lang, G.A., Iwakuma, T., Suh, Y.A., Liu, G., Rao, V.A., Parant, J.M., Valentin-Vega, Y.A., Terzian, T., Caldwell, L.C., Strong, L.C., et al. (2004). Gain of function of a p53 hot spot mutation in a mouse model of Li-Fraumeni syndrome. Cell *119*, 861–872.

Lin, S.J., Defossez, P.A., and Guarente, L. (2000). Requirement of NAD and SIR2 for life-span extension by calorie restriction in Saccharomyces cerevisiae. Science *289*, 2126–2128.

Matoba, S., Kang, J.G., Patino, W.D., Wragg, A., Boehm, M., Gavrilova, O., Hurley, P.J., Bunz, F., and Hwang, P.M. (2006). p53 regulates mitochondrial respiration. Science *312*, 1650–1653.

Memon, R.A., Grunfeld, C., Moser, A.H., and Feingold, K.R. (1994). Fatty acid synthesis in obese insulin resistant diabetic mice. Horm. Metab. Res. *26*, 85–87.

Mills, A.A., Zheng, B., Wang, X.J., Vogel, H., Roop, D.R., and Bradley, A. (1999). p63 is a p53 homologue required for limb and epidermal morphogenesis. Nature *398*, 708–713.

Olive, K.P., Tuveson, D.A., Ruhe, Z.C., Yin, B., Willis, N.A., Bronson, R.T., Crowley, D., and Jacks, T. (2004). Mutant p53 gain of function in two mouse models of Li-Fraumeni syndrome. Cell *119*, 847–860.

Purushotham, A., Schug, T.T., Xu, Q., Surapureddi, S., Guo, X., and Li, X. (2009). Hepatocyte-specific deletion of SIRT1 alters fatty acid metabolism and results in hepatic steatosis and inflammation. Cell Metab. *9*, 327–338.

Rodgers, J.T., and Puigserver, P. (2007). Fasting-dependent glucose and lipid metabolic response through hepatic sirtuin 1. Proc. Natl. Acad. Sci. USA *104*, 12861–12866.

Rodgers, J.T., Lerin, C., Haas, W., Gygi, S.P., Spiegelman, B.M., and Puigserver, P. (2005). Nutrient control of glucose homeostasis through a complex of PGC-1alpha and SIRT1. Nature *434*, 113–118.

Rogina, B., and Helfand, S.L. (2004). Sir2 mediates longevity in the fly through a pathway related to calorie restriction. Proc. Natl. Acad. Sci. USA *101*, 15998–16003.

Shaw, R.J., Kosmatka, M., Bardeesy, N., Hurley, R.L., Witters, L.A., DePinho, R.A., and Cantley, L.C. (2004). The tumor suppressor LKB1 kinase directly activates AMP-activated kinase and regulates apoptosis in response to energy stress. Proc. Natl. Acad. Sci. USA *101*, 3329–3335.

Shaw, R.J., Lamia, K.A., Vasquez, D., Koo, S.H., Bardeesy, N., Depinho, R.A., Montminy, M., and Cantley, L.C. (2005). The kinase LKB1 mediates glucose homeostasis in liver and therapeutic effects of metformin. Science *310*, 1642–1646.

Su, X., Paris, M., Gi, Y.J., Tsai, K.Y., Cho, M.S., Lin, Y.L., Biernaskie, J.A., Sinha, S., Prives, C., Pevny, L.H., et al. (2009). TAp63 prevents premature aging by promoting adult stem cell maintenance. Cell Stem Cell *5*, 64–75.

Su, X., Chakravarti, D., Cho, M.S., Liu, L., Gi, Y.J., Lin, Y.L., Leung, M.L., El-Naggar, A., Creighton, C.J., Suraokar, M.B., et al. (2010). TAp63 suppresses metastasis through coordinate regulation of Dicer and miRNAs. Nature *467*, 986–990.

Suh, E.K., Yang, A., Kettenbach, A., Bamberger, C., Michaelis, A.H., Zhu, Z., Elvin, J.A., Bronson, R.T., Crum, C.P., and McKeon, F. (2006). p63 protects the female germ line during meiotic arrest. Nature *444*, 624–628.

Takemori, K., Kimura, T., Shirasaka, N., Inoue, T., Masuno, K., and Ito, H. (2011). Food restriction improves glucose and lipid metabolism through Sirt1 expression: a study using a new rat model with obesity and severe hypertension. Life Sci. *88*, 1088–1094.

Towler, M.C., and Hardie, D.G. (2007). AMP-activated protein kinase in metabolic control and insulin signaling. Circ. Res. *100*, 328–341.

Vaziri, H., Dessain, S.K., Ng Eaton, E., Imai, S.I., Frye, R.A., Pandita, T.K., Guarente, L., and Weinberg, R.A. (2001). hSIR2(SIRT1) functions as an NAD-dependent p53 deacetylase. Cell *107*, 149–159.

Viollet, B., Andreelli, F., Jørgensen, S.B., Perrin, C., Geloen, A., Flamez, D., Mu, J., Lenzner, C., Baud, O., Bennoun, M., et al. (2003). The AMP-activated

protein kinase alpha2 catalytic subunit controls whole-body insulin sensitivity. J. Clin. Invest. *111*, 91–98.

Wang, R.H., Sengupta, K., Li, C., Kim, H.S., Cao, L., Xiao, C., Kim, S., Xu, X., Zheng, Y., Chilton, B., et al. (2008). Impaired DNA damage response, genome instability, and tumorigenesis in SIRT1 mutant mice. Cancer Cell *14*, 312–323.

Woods, A., Johnstone, S.R., Dickerson, K., Leiper, F.C., Fryer, L.G., Neumann, D., Schlattner, U., Wallimann, T., Carlson, M., and Carling, D. (2003). LKB1 is the upstream kinase in the AMP-activated protein kinase cascade. Curr. Biol. *13*, 2004–2008.

Yang, A., Schweitzer, R., Sun, D., Kaghad, M., Walker, N., Bronson, R.T., Tabin, C., Sharpe, A., Caput, D., Crum, C., and McKeon, F. (1999). p63 is essential for regenerative proliferation in limb, craniofacial and epithelial development. Nature *398*, 714–718.

Yang, A., Zhu, Z., Kapranov, P., McKeon, F., Church, G.M., Gingeras, T.R., and Struhl, K. (2006). Relationships between p63 binding, DNA sequence, transcription activity, and biological function in human cells. Mol. Cell *24*, 593–602.

Zang, M., Xu, S., Maitland-Toolan, K.A., Zuccollo, A., Hou, X., Jiang, B., Wierzbicki, M., Verbeuren, T.J., and Cohen, R.A. (2006). Polyphenols stimulate AMP-activated protein kinase, lower lipids, and inhibit accelerated atherosclerosis in diabetic LDL receptor-deficient mice. Diabetes *55*, 2180–2191.